AIP | Applied Physics Letters

Fabrication and magnetic properties of ultrathin Fe nanowire arrays

X. Y. Zhang, G. H. Wen, Y. F. Chan, R. K. Zheng, X. X. Zhang, and N. Wang

Citation: Applied Physics Letters **83**, 3341 (2003); doi: 10.1063/1.1621459
View online: http://dx.doi.org/10.1063/1.1621459
View Table of Contents: http://scitation.aip.org/content/aip/journal/apl/83/16?ver=pdfcov
Published by the AIP Publishing

Fabrication and magnetic properties of ultrathin Fe nanowire arrays

X. Y. Zhang, G. H. Wen, Y. F. Chan, R. K. Zheng, X. X. Zhang, and N. Wang[a)]
Department of Physics, Institute of Nano Science and Technology, The Hong Kong University of Science and Technology, Clear Water Bay, Hong Kong, China

(Received 2 June 2003; accepted 29 August 2003)

Ultrathin Fe nanowire (about 5 nm in diameter) arrays have been fabricated by electrodeposition using anodic porous alumina templates. These ultrathin nanowires exhibited uniaxial anisotropy and a quite large coercivity (4190 Oe) at 5 K. In addition, the field needed to saturate the magnetization, when the field was applied perpendicularly to the easy axis, was much larger than the shape anisotropy field ($2\pi M_S$). This saturation field increased with decreasing temperature. We believed that this enhanced saturation field was mainly due to the contribution of the surface spins. © *2003 American Institute of Physics.* [DOI: 10.1063/1.1621459]

In recent years, there has been increasing interest in the fabrication of one-dimensional nanostructures because of their potential utilization in many fields.[1–4] Magnetic nanowire arrays are of great interest for both fundamental science and potential applications in, such as, high-density perpendicular magnetic recording media and nanosensors.[5–8] The synthesis and precise control of such a magnetic nanostructure on a large scale is a challenging issue in materials science. One strategy is to electrodeposit the magnetic nanowires into the nanochannels of anodic porous alumina templates, which have been investigated previously by many groups.[6–13]

The porous alumina substrates were fabricated by anodizing pure aluminum foils (purity 99.999%) in a sulfuric acid solution. Prior to anodizing, the aluminum foils were annealed at 500 °C for 2 h in order to homogenize the microstructures and reduce the density of defects in the foils. This was essential for the formation of high quality nanochannels over large areas in the alumina substrates. Subsequently, the foils were electropolished in the solution of C_2H_5OH mixed with $HClO_4$ (9:1 in volume) in order to obtain a high quality of flat surfaces. Then, anodization was carried out under a condition of constant cell voltage of 5.5 V in a 3.5 M H_2SO_4 solution. The temperature was kept constant at 0 °C. The preformed alumina layer was removed by phosphoric acid and chromic acid, and then the aluminum foil with a fresh and clean surface was anodized again under the same anodizing condition. After the anodization, Fe nanowires were prepared by ac (14 V, 50 Hz) electrodeposition in the solution of $FeSO_4 \cdot 7H_2O$ (45 g/l) + H_3BO_3 (50 g/l) with a *p*H value of 3.5. The temperature for the electrodeposition was 25 °C.

Figure 1(a) shows the x-ray diffraction (XRD) spectrum of the Fe nanowire arrays after completely dissolving the aluminum substrate in a $HgCl_2$ saturated solution. The diffraction peaks of (110), (200), and (211) are clearly distinguishable, and match perfectly with the bcc Fe structure with a lattice constant of $a = 0.2866$ nm. Figure 1(b) is a plan-view transmission electron microscope (TEM) image showing the typical microstructure of the porous alumina templates. The diameters and the separation distances of the pores are about 5 and 15 nm, respectively. Figure 1(c) is a typical cross-sectional view of the template filled with Fe nanowires whose diameters and lengths are about 5 nm and 2 μm, respectively. Fe nanowires are well aligned indicating the nanochannels in the substrate are uniformly distributed through the entire substrates. Since the TEM sample was sectioned along a certain direction, only some of the nanowires were imaged in this figure. Figure 1(d) shows an isolated Fe nanowire after completely dissolving the alumina template and dispersing the sample on a carbon supporting film. Most Fe nanowires observed were single crystalline. The selected-area electron diffraction pattern [inset in Fig. 1(d)] taken from this nanowire was indexed as the [110] zone axis of bcc Fe structure. This result was consistent with that obtained from the XRD measurement. Using similar method, we have also synthesized Ni and Ni–Co alloy nanowires in the templates. Their structure and morphology were very

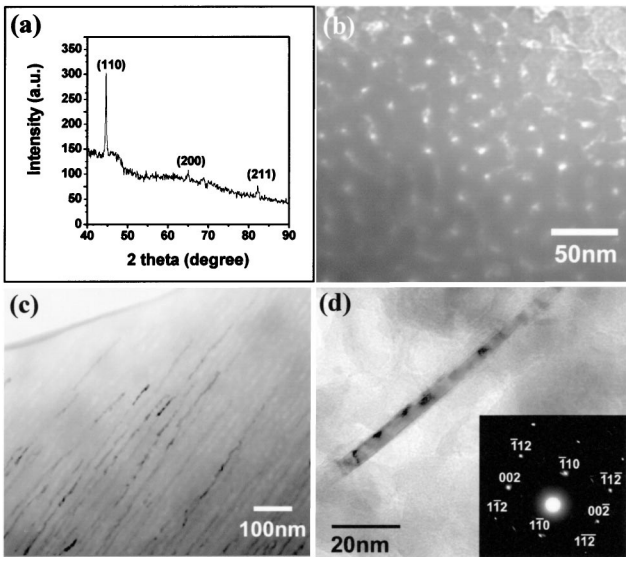

FIG. 1. (a) XRD result taken from Fe nanowire arrays. (b) TEM image of the alumina template with 5 nm diameter pores. (c) Cross-sectional view of the template filled with Fe nanowire arrays. (d) An isolated Fe nanowire with a diameter of about 5 nm and its selected-area electron diffraction pattern (inset).

a)Author to whom correspondence should be addressed; electronic mail: phwang@ust.hk

similar to the Fe nanowires illustrated earlier.

To understand the magnetism in the magnetic nanowire arrays, hysteresis loops have been measured in a wide temperature range from 5 to 350 K. Because of the very larger length-to-diameter ratio (~ 200) of Fe nanowires, it is expected that the effective magnetic anisotropy is dominated by the shape anisotropy $2\pi M_S$, where M_S is the saturation magnetization of the materials. This means that the easy axis of magnetization is along the wire axis. Figure 2(a) shows the hysteresis loops obtained from Fe nanowire arrays with the applied external magnetic field perpendicular to the sample plane (parallel to the wire axis) and parallel to the sample plane (perpendicular to the wire axis) at 300 K. It should be pointed out that the magnetization data plotted here are the values extracted by using $M = M_{\text{tot}} - \chi H$, where M_{tot} is the measured value and χ is the diamagnetic susceptibility of the templates, a small negative constant. It is clearly seen from Fig. 2(a) that the magnetic easy axis is along the wire axis, which can be easily saturated as we expected. From the hysteresis loop data, the parameters that describe the hysteresis loop behavior are obtained: $H_{c\perp} = 1470$ Oe, $H_{c\parallel} = 530$ Oe, $M_{r\perp}/M_{s\perp} = 0.88$ and $M_{r\parallel}/M_{s\parallel} = 0.10$. Previous studies show that the coercivity of magnetic nanowires depends strongly on their diameters.[11,12] At 300 K, there is a critical diameter (d_C) for Fe wires at which the maximum coercivety appears. The fact that coercivity decreases with decreasing the diameter of the wires, if the wire diameter $d < d_C$, is suggested to be due to the thermal effects.[14] The reported d_C for Fe nanowires is 13 nm, and the largest value of coercivity is 2640 Oe.[12] Since the diameters of our Fe nanowires are much smaller than d_C, it is expected that the value of coercivity obtained at 300 K is smaller than that reported by the others.[11–13] However, the diameter dependence of the coercivity measured at a low temperature of 5 K shows a very different behavior because no maximum has been observed, i.e., the coercivity increases monotonically with decreasing the diameter.[11,12] The smallest diameter of Fe nanowire arrays reported by Menon *et al.* is 9 nm.[12] These nanowires exhibit a coercive field of 3700 Oe at 5 K. The diameter of Fe nanowires prepared in this work, which show a higher coercive field of 4190 Oe at 5 K is about 5 nm, much smaller than 9 nm. From a simple extrapolation of the data shown in Fig. 3(b) in Ref. 12 (the coercivity as a function of diameter measured at 5 K), we find that the coercivity will be roughly about 4200 Oe for the 5 nm Fe nanowires, indicating that our results are qualitatively in line with what reported previously.[11,12]

Figure 2(b) shows the temperature dependence of the coercivity with the field applied perpendicularly to the sample plane (parallel to wire axis). It is manifest that $H_{c\perp}$ decreases with increasing temperature, from 4190 Oe at 5 K to 1470 Oe at 300 K, indicating a much stronger temperature-dependent characteristic than that reported in Ref. 11 for Fe nanowires with large diameters. By considering the thermal effect in nanowire structure, the coercivity can be described by[11]

$$H_C = H_A\left\{1 - \left[\frac{k_B T}{K_u V}\ln(f_0\tau)\right]^{1/m}\right\}, \tag{1}$$

where H_A is the anisotropy field, K_u and V are the uniaxial anisotropy constant and volume of the wire; k_B is the Boltzmann constant, $f_0 (\sim 10^9$ Hz), and τ is the attempt frequency and relaxation time. In the inset to Fig. 2(b), the coercivity data are replotted as a function of $T^{1/2}$, where the line is the linear fit of the data. Obviously, the coercivity has $T^{1/2}$ dependence, i.e., $m = 2$. Actually, $m = 2$ is corresponding to the case of aligned, noninteracting Stoner–Wohlfarth particles, where the reversal of magnetization is coherent. The coherent reversal of magnetic moment in 5 nm nanowires should be expected.[11] Inspection of the high-field magnetization data obtained at 300 K reveals that the magnetization saturates at about 1.2 T for the field parallel to the sample plane (or perpendicular to the wire axis). This saturation field (H_S) is usually very close to the anisotropy field (H_A) in nanowires.[11] But this value is larger than that reported for the Fe wires with larger diameters and also lager than the theoretical value ($2\pi M_S = 1.073$ T) of the shape anisotropy in nanowire structure for Fe at 300 K. Figure 3(a) shows magnetization curves for the applied field parallel to the sample plane (or perpendicular to the wire axis) obtained at different temperatures. It is obvious that the saturation field which is

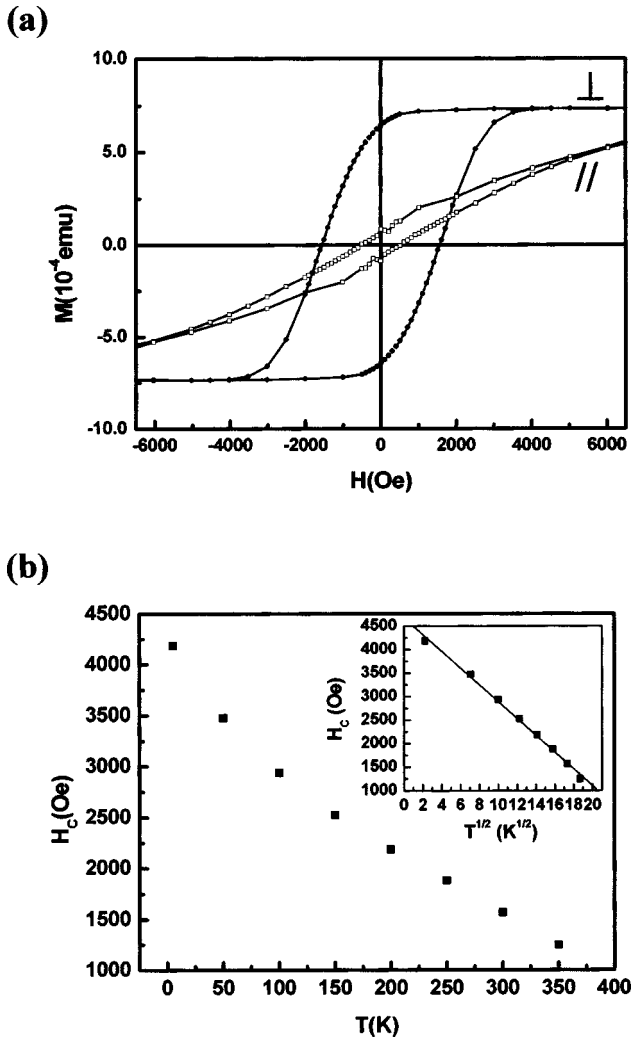

FIG. 2. (a) The hysteresis loops of the Fe nanowires at 300 K. "⊥" indicates the magnetic field applied perpendicularly to the sample surface, i.e., parallel to the nanowire axes. "∥" denotes the magnetic field parallel to the sample surface. (b) The temperature dependence of the coercivity of Fe nanowires for the field applied perpendicular to the sample plane. The inset is the replot of H_C as a function of $T^{1/2}$.

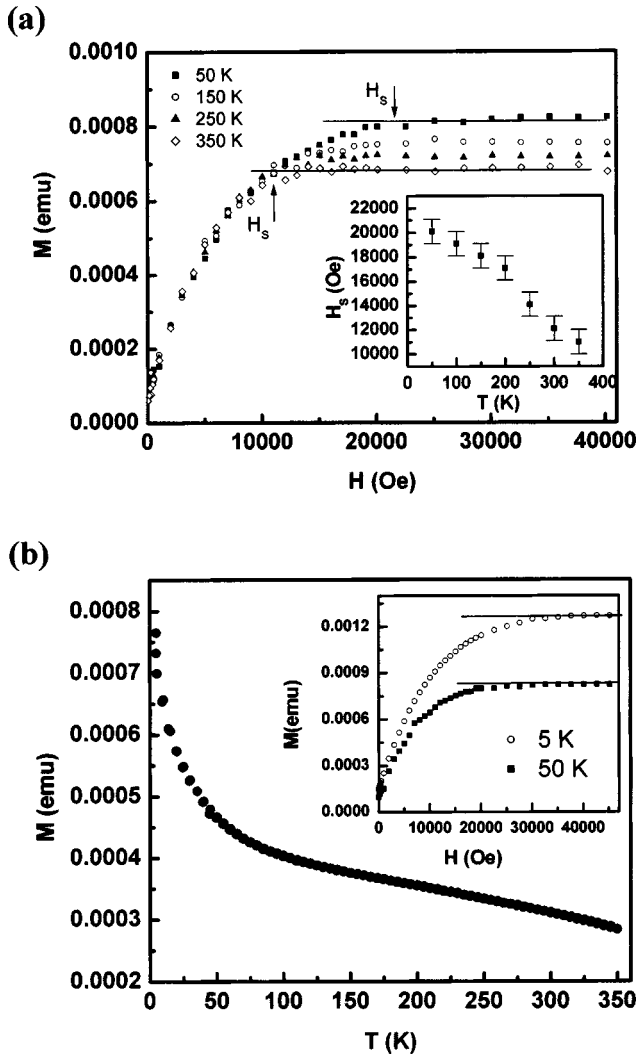

FIG. 3. (a) Plot of magnetization vs field obtained at different temperatures, where the field is parallel to the sample plane (or perpendicular to the wire axis). The inset shows the estimated saturation field vs temperature and the saturation field plotted as a function of temperature. (b) The temperature-dependent magnetization with 1 T magnetic field applied perpendicularly to the sample plane (or parallel to the wire axis). The inset reveals the magnetization versus field obtained at 5 and 50 K. It is clear that the surface spins are much difficult to be aligned at low temperatures.

larger than $2\pi M_S$ increases with decreasing temperature. The estimated saturation field decreases monotonically with increasing temperature [inset to Fig. 3(a)].

From the strong temperature dependence of coercivity and the saturation magnetic field [inset to Fig. 3(a)], the heuristic understanding of the observation is that except the contribution of the shape anisotropy ($2\pi M_S$) to the saturation field, there must be another contribution that makes the magnetization difficult to be saturated. In the present case, the diameters of the Fe wires are about 5 nm, much smaller than the coherent diameter $d_{\mathrm{coh}}=11$ nm for Fe.[11] Therefore, the reversal of the magnetization should be coherent if the wire is free of local imperfections.[11] If the reversal of magnetization is coherent, the saturation field should equal the anisotropy field, which is dominated by the demagnetization field $2\pi M_S$ in very long and narrow wires. Here, we observe that the saturation field is much larger than $2\pi M_S$ in the whole temperature range (5–350 K), which might be attributed to the surface spins of the very narrow wires. If we assume that the surface spin is about two atomic layers, the percentage of the surface spins will be ~20% for the Fe nanowire with a diameter of 5 nm. Due to the reduction of the coordination and the interface between Fe wire and the template, the magnetic configuration of the surface spins must be different from that in the bulk, which must affect the magnetic behavior of the wires. Surface-spin effect in nanostructured magnetic materials has been well known and studied intensively.[15,16] Surface spins are normally very difficult to be aligned, even in a very larger magnetic field as observed in magnetic nanoparticles.[15,16] In some cases, surface spins form a spin-glass-like layer.[15,16] With increasing the diameters of the wires, the surface spin contribution becomes weaker and weaker; the saturation of magnetization will be dominated by the shape anisotropy ($2\pi M_S$) as observed by Sellmyer *et al.*[11]

If the surface spins form a spin-glass-like layer in our ultrathin Fe wires, it will be in a frozen state at low temperatures and become superparamagnetic (or paramagnetic) above the freezing temperature. Therefore, it is difficult to reach the saturation state in the whole temperature range. The existence of the surface spin contribution can be observed from the low temperature magnetization curves and the temperature dependent magnetization. Figure 3(b) reveals the temperature dependent magnetization measured with 1 T magnetic field applied perpendicularly to the sample plane (or parallel to the wire axis). Clearly, there is a strong temperature-dependent magnetic contribution at low temperatures superimposing to the weak temperature-dependent magnetization resulted from the wire cores (bcc Fe). This can also be observed from the field-dependent magnetization measured at 5–50 K [inset to Fig. 3(b)].

This work was supported by grants from the Research Grant Council of Hong Kong (Project Nos. HKUST6151/01P and 6165/01P).

[1] S. Iijima, Nature (London) **354**, 56 (1991).
[2] M. H. Dvoret, D. Esteve, and C. Urbina, Nature (London) **360**, 547 (1992).
[3] H. Dai, E. W. Wong, Y. Z. Lu, S. Fan, and C. M. Lieber, Nature (London) **375**, 769 (1995).
[4] A. P. Alivisatos, Science (Washington, DC, U.S.) **271**, 933 (1996).
[5] K. Uosaki, K. Okazaki, H. Kita, and H. Takahashi, Anal. Chem. **62**, 652 (1990).
[6] T. M. Whitney, J. S. Jiang, P. C. Searson, and C. L. Chien, Science (Washington, DC, U.S.) **261**, 1316 (1993).
[7] C. Z. Zhang and J. C. Lodder, J. Magn. Magn. Mater. **88**, 236 (1990).
[8] D. Almawlawi, N. Coombs, and M. Moskovits, J. Appl. Phys. **70**, 4421 (1991).
[9] R. Ferré, K. Ounadjela, J. M. George, L. Piraux, and S. Dubois, Phys. Rev. B **56**, 14 066 (1997).
[10] M. Zheng, L. Menon, H. Zeng, Y. liu, S. Bandyopadhyay, R. D. Kirby, and D. J. Sellmyer, Phys. Rev. B **62**, 12 282 (2000).
[11] D. J. Sellmyer, M. Zheng, and R. Skomski, J. Phys.: Condens. Matter **13**, R433 (2001).
[12] L. Menon, M. Zheng, H. Zeng, S. Bandyopadhyay, and D. J. Sellmyer, J. Electron. Mater. **29**, 510 (2000).
[13] F.-Y. Li, L. Zhang, and R. M. Metzger, Chem. Mater. **10**, 2470 (1998).
[14] B. D. Cullity, *Introduction to Magnetic Materials* (Addison-Wesley, New York, 1972), pp. 386–387.
[15] R. H. Kodama, S. A. Makhlouf, and A. E. Berkowitz, Phys. Rev. Lett. **79**, 1393 (1997); R. H. Kodama, A. E. Berkowitz, E. J. McNiff, Jr., and S. Foner, *ibid.* **77**, 394 (1996).
[16] B. Martínez, X. Obradors, L. Balcells, A. Rouanet, and C. Monty, Phys. Rev. Lett. **80**, 181 (1998), and references therein.